

## MIT Open Access Articles

*Stretchable Polymeric Multielectrode  
Array for Conformal Neural Interfacing*

The MIT Faculty has made this article openly available. **Please share**  
how this access benefits you. Your story matters.

**Citation:** Guo, Liang, Mingming Ma, Ning Zhang, Robert Langer, and Daniel G. Anderson. "Stretchable Polymeric Multielectrode Array for Conformal Neural Interfacing." *Advanced Materials* 26, no. 9 (October 22, 2013): 1427–1433.

**As Published:** <http://dx.doi.org/10.1002/adma.201304140>

**Publisher:** Wiley Blackwell

**Persistent URL:** <http://hdl.handle.net/1721.1/101128>

**Version:** Author's final manuscript: final author's manuscript post peer review, without publisher's formatting or copy editing

**Terms of use:** Creative Commons Attribution-Noncommercial-Share Alike





Published in final edited form as:

*Adv Mater.* 2014 March 5; 26(9): 1427–1433. doi:10.1002/adma.201304140.

## Stretchable Polymeric Multielectrode Array for Conformal Neural Interfacing

**Dr. Liang Guo,**

David H. Koch Institute for Integrative Cancer Research, Massachusetts Institute of Technology, Cambridge, Massachusetts 02139, USA

**Dr. Mingming Ma,**

David H. Koch Institute for Integrative Cancer Research, Massachusetts Institute of Technology, Cambridge, Massachusetts 02139, USA

**Dr. Ning Zhang,**

David H. Koch Institute for Integrative Cancer Research, Massachusetts Institute of Technology, Cambridge, Massachusetts 02139, USA

**Prof. Robert Langer,** and

David H. Koch Institute for Integrative Cancer Research, Department of Chemical Engineering, Division of Health Science and Technology, Institute for Medical Engineering and Science, Massachusetts Institute of Technology, Cambridge, Massachusetts 02139, USA

**Prof. Daniel G. Anderson**

David H. Koch Institute for Integrative Cancer Research, Department of Chemical Engineering, Division of Health Science and Technology, Institute for Medical Engineering and Science, Massachusetts Institute of Technology, Cambridge, Massachusetts 02139, USA

Daniel G. Anderson: dgander@mit.edu

### Abstract

Highly stretchable neural interface of concurrent robust electrical and mechanical properties is developed with a conducting polymer film as the sole conductor for both electrodes and leads. This neural interface offers benefits of conducting polymer electrodes in a demanding stretchable format, including low electrode impedance and high charge injection capacity, due to large electroactive surface area of the electrode.

### Keywords

Conducting polymer; polypyrrole; stretchable multielectrode array; conformal; neural interface

Conducting polymers are often employed as coatings on smooth metal electrodes to improve the electrode performance with respect to the signal-to-noise ratio (SNR) for neural

Correspondence to: Daniel G. Anderson, dgander@mit.edu.

Dr. L. Guo is now at the Department of Electrical and Computer Engineering, Department of Neuroscience, The Ohio State University, Columbus, Ohio 43210, USA

Supporting Information is available online from Wiley InterScience or from the author.

recording, charge injection capacity for neural stimulation, and inducement of neural growth for electrode-tissue integration.<sup>[1-5]</sup> The enlarged electrochemical surface area of coated neural electrodes leads to low electrode impedance and high charge storage capacity, while the physicochemical properties of the coating offer a conducive micro/nano environment for neurite growth.<sup>[5-8]</sup> However, conventional conducting polymers are mechanically brittle.<sup>[1-3]</sup> Flexible neural electrode arrays bearing conducting polymer electrodes have been developed,<sup>[9-11]</sup> but these are not stretchable, which is a requirement in many neural applications, such as epimysial interfacing. Using a flat conducting polymer film as the sole conductor, here we develop a highly stretchable neural interface with concurrent excellent electrical and mechanical properties. To our knowledge, this is the first neural interface that can offer the benefits of conducting polymer electrodes in a demanding stretchable format, including low electrode impedance and high charge injection capacity, as well as the first stretchable neural interface that uses a conducting polymer film as the sole conductor.<sup>[1-5,9-11,13-15,31]</sup>

Polypyrrole (PPy) and poly(3,4-ethylenedioxythiophene) (PEDOT) are the most widely used polymer coatings for neural electrodes, due to their electrical and mechanical properties and biocompatibility.<sup>[1-5,11]</sup> Recently, a polypyrrole/polyol-borate composite was synthesized which offered superior mechanical strength and flexibility with favorable electrical conductivity.<sup>[12]</sup> Here we developed a stretchable multielectrode array, directly, using a new polypyrrole/polyol-borate composite film as the sole conductor for both electrodes and leads, in contrast with the conventional approach of incorporating conducting polymers only through coating on non-stretchable metal electrodes.<sup>[1-5,11]</sup> The resulting stretchable polymeric multielectrode array (SPMEA) was stretchable up to  $(22.84 \pm 1.64)\%$  uniaxial tensile strain with minimal losses in electrical conductivity.

With a hydrophobic diol (PolyCaprolactone-block-polyTetrahydrofuran-block-polyCaprolactone, PCTC,  $\text{CL}_x\text{-THF}_y\text{-CL}_z$ ,  $x + z \approx 11$ ,  $y \approx 17$ .<sup>[30]</sup>) providing good electrical conductivity, the PPy/PCTC composite film was synthesized following a published procedure.<sup>[12]</sup> Briefly, an organic solvent synthesis system with a three-electrode electrochemical cell was used.<sup>[12,16]</sup> A glass microscope slide ( $40 \text{ mm} \times 25 \text{ mm} \times 1 \text{ mm}$ ) sputtered with a 25 nm platinum (Pt) seed layer served as the working electrode, on which the PPy/PCTC film was synthesized. Figure 1 shows the chemical structure, representative photographs and electromechanical properties of the resulting PPy/PCTC films in their dry state. The face contacting the Pt electrode had a shiny smooth-metal-like surface, whereas the other face was rough. The material had a conductivity of  $116.3 \pm 7.8 \text{ S cm}^{-1}$  ( $n = 4$ ) as measured by a standard four-point probe method, which is typical for electrochemically synthesized PPy samples.<sup>[1,2]</sup> The dry film was able to withstand a uniaxial tensile strain up to  $(25.21 \pm 2.50)\%$  ( $n = 4$ ) (in comparison, a water-saturated film had an ultimate tensile strain of 52.5%, see Figure S3.). The ultimate tensile strength was  $145.56 \pm 25.31 \text{ MPa}$ , indicating that this polymeric material was stronger than most engineering plastics and comparable to some metal materials such as aluminum.<sup>[12,16]</sup> The elastic modulus of the dry PPy/PCTC was  $153.87 \pm 25.31 \text{ MPa}$ , within the range of typical PPy films<sup>[13]</sup> and a few orders of magnitude lower than those of noble metals used for neural electrodes.<sup>[21]</sup> Interestingly, the electrical resistance increased linearly with the tensile strain but peaked at an increase of only  $(23.99 \pm 3.49)\%$  at the ultimate tensile strain.<sup>[14]</sup> In contrast, most

freestanding metal thin films rupture at a strain of around 1%<sup>[17]</sup> and experience a dramatic increase in resistance, up to a few folds, at the rupture strain.<sup>[18]</sup> Therefore, these mechanical and electrical properties make the PPy/PCTC material an attractive conductor for building stretchable neural interfaces.

The PPy/PCTC film is essentially plastic, with an elastic deformation range of only ~5% (Figure 1c). To create a stretchable interconnect using the PPy/PCTC film as the conductor, we embedded the plastic PPy/PCTC interconnect in an insulating elastomer body.<sup>[13,14]</sup> We hypothesized that the bulk elastomer will retain its elasticity, even if the embedded PPy/PCTC interconnect undergoes plastic deformation at tensile strains beyond 5%. Such a device was fabricated in a 20 mm × 1 mm × 150 μm sandwiched structure comprising a 125 μm thick polydimethylsiloxane (PDMS) substrate, a 15 μm thick PPy/PCTC film and a 10 μm thick passivation PDMS layer. For electrical probing, the PPy/PCTC was exposed at both ends of the interconnect. In order to improve the device's physical integrity and mechanical performance, a special technique<sup>[20]</sup> was incorporated in the fabrication process to form permanent chemical bonding between the PPy/PCTC film and PDMS substrate. Such permanent bonding of the conductor to an elastomer substrate is critical for the yield of a high rupture strain,<sup>[19,14]</sup> but is not achievable with noble metal thin films until very recently.<sup>[18,21,32]</sup> Electromechanical testing results of the stretchable interconnect are represented in Figure 2. Stretchable interconnects ruptured at a tensile strain of  $(22.84 \pm 1.64)\%$  ( $n = 4$ ), which is not statistically significant from that of the dry PPy/PCTC film (Student's T-Test,  $p = 0.17104$ ), indicating the presence of a bonded PDMS substrate had no promotive effect on the rupture strain of the PPy/PCTC film. The linear relationship between electrical resistance and tensile strain was preserved,<sup>[14]</sup> though more noise was observed. The electrical resistance only had an increase of  $(16.10 \pm 0.92)\%$  at the rupture strain (comparing with that of the dry PPy/PCTC film, Student's T-Test,  $p = 0.01689$ ), implying the PDMS encapsulation slightly muted the electrical resistance increase, as manifested by the lower slope of the fitting line (also see Supporting Information).

At 20% cyclic strain (Figures 2c and 2d), the specimen ruptured after 7.5 cycles. When a specimen (without top PDMS encapsulation) that had undergone one cycle of 20% strain was inspected under an SEM, a few micro-cracks were found in the top surface, with orientations perpendicular to the direction of stretch (Figure S4). This observation could explain the specimen's mechanism of failure. Cyclic loading could have resulted in the continuous formation of micro-cracks in the PPy/PCTC film and ultimately led to rupture of the specimen. The progressive development of micro-cracks in the PPy/PCTC film may also partially explain the polynomial drift of the baseline resistance in Figure 2d.<sup>[14]</sup> Another major contribution to this baseline drift may be progressive plastic deformation of the PPy/PCTC film, which was clearly observed in Figure 2c. With a thickness ratio of 1:10 between the PPy/PCTC film and bulk PDMS, after the first cycle, the specimen was permanently elongated by ~8%, thereafter progressively elongating to ~12% after the seventh cycle. A similar phenomenon was observed on a specimen subjected to a 10% cyclic strain (Figure S5), which survived ten cycles and whose final length at relaxation increased by ~4.2%. It is expected that, as the thickness ratio between the PPy/PCTC film and bulk PDMS decreases, the stretchable interconnect will retract to a length closer to its initial value and the permanently deformed PPy/PCTC film will corrugate with higher amplitudes at relaxed

state.<sup>[13,14]</sup> In Figure 2d, in each cycle, the resistance changed linearly with strain, with uniform overshoot amplitudes at 20% strains across the cycles.<sup>[14]</sup> At the rupture point, the baseline resistance only increased by ~50%. These excellent electromechanical properties render the stretchable interconnect a promising candidate for stretchable neural interfaces.

A fully packaged SPMEA was fabricated as shown in Figure 3a. The fabrication process (refer to the *Experimental* section and also see Figure S6) was designed such that the rougher surface of the PPy/PCTC film served as the electrode surface (top inset in Figure 3a). Diameters of the surface micro-grains were in the range of 1–5  $\mu\text{m}$  and could be controlled by the electroplating current density. A lower current density yields finer surface micro-grains and produces PPy/PCTC films with better electromechanical properties. Electrical impedance spectroscopy (Figure 3b) of the PPy/PCTC electrodes revealed flatter impedance amplitudes across the frequency range of 0.1 Hz ~ 100 kHz with better low frequency (below 80 Hz) responses than those of a Pt disc electrode (see Figure S9) of the same geometric size. Phase responses (Figure 3c) indicated that the PPy/PCTC electrodes were more resistive at frequencies below 1 kHz. Thus, this type of electrodes is more suitable for recording local field potentials (LFPs) such as electromyograms (EMG), electrocardiograms (ECG), electrocorticograms (ECoG) and electroencephalograms (EEG). Therefore, we demonstrated the recording capability of the SPMEA in an acute epimysial recording experiment using a rat model (Figure 3d). The device successfully measured multichannel EMGs from the lateral gastrocnemius muscle, following a mechanical squeeze of the sciatic nerve. A representative recording trace is shown in Figure 3e.

To characterize the stimulation capability of the SPMEA, we performed cyclic voltammetry (CV) at both slow ( $50 \text{ mV s}^{-1}$ ) and fast ( $1 \text{ V s}^{-1}$ ) voltage sweeps within the water electrolysis window ( $-0.6 \text{ V} \sim 0.8 \text{ V}$ ). The slow CV uncovered an impressive cathodic charge storage capacity ( $\text{CSC}_c$ ) of  $48.8 \text{ mC cm}^{-2}$  of the PPy/PCTC electrode, as compared with  $5.0 \text{ mC cm}^{-2}$  of the Pt electrode (Figure 4a). The PPy/PCTC's  $\text{CSC}_c$  is better than those of other common stimulation electrode materials, such as iridium oxide ( $28.8 \text{ mC cm}^{-2}$ ), and nears the best value reported for PEDOT film coated electrodes ( $75.6 \text{ mC cm}^{-2}$ ).<sup>[22,29]</sup> The charge injection capacity was evaluated by the fast CV (Figure 4b), which identifies the charges immediately available at the electrode surface when the electrode is driven by short stimulation pulses. With a cathodic charge transfer of  $3.9 \text{ mC cm}^{-2}$  in the fast CV mode, the PPy/PCTC electrode still outperformed many other common electrode materials. It has been reported that PPy electrodes offer a poor charge injection rate capability.<sup>[22]</sup> This research is focused on the electrical stimulation of denervated skeletal muscles, which requires long stimulation pulses of hundreds of milliseconds.<sup>[23]</sup> From Figure 4b, a  $3.9 \text{ mC}$  charge can be delivered in the cathodic phase within 1 s using a  $1 \text{ cm}^2$  PPy/PCTC electrode, *i.e.*, an average cathodic charge injection of  $1.17 \text{ mC}$  using a 300 ms pulse. Thus, with a much smaller size than smooth metal electrodes, PPy/PCTC electrodes are sufficient to safely activate a denervated muscle epimysially.<sup>[24]</sup>

Prior work on stretchable neural interfaces employed noble metal thin film conductors almost exclusively.<sup>[21,25-27,11]</sup> Although these devices had adequate electrical properties at low strain loading, the electrical performance significantly worsened at high strain loading. Moreover, these electrodes still required modification with conducting polymers to improve

their electrical performance.<sup>[11]</sup> A flexible polymeric microelectrode array was developed using PEDOT as the sole conductor,<sup>[9]</sup> but the device was not stretchable. Other attempts have been made to improve the mechanical properties of CPs by creating blends, however, despite improved mechanical properties, neural electrodes made of such conducting polymer-elastomer blends suffer from low conductivity, particularly at high strain loadings.<sup>[10]</sup> Therefore, obtaining concurrently excellent mechanical and electrical properties of conducting polymers still remains a challenge.<sup>[2]</sup> This materials challenge has been addressed directly by a highly stretchable conducting polymer PPy/PCTC described here. This stretchable neural interface has the inherent benefits of conducting polymer electrodes. The stretchability can be further improved by using a pre-stretched PDMS substrate to create highly corrugated structures in the PPy/PCTC film.<sup>[13,14]</sup> The common delamination problem of conducting polymer coatings on metal electrodes was thus avoided. Additional benefits of conducting polymers can be exploited further in the SPMEA design, *e.g.*, capabilities of releasing anti-inflammatory drugs and/or growth factors can be incorporated into the PPy/PCTC electrode, combining both electrical and biochemical means to improve the performance of neural electrodes.<sup>[1-4]</sup> Lastly, PPy/PCTC is inexpensive and easy to synthesize, offering a cost-effective solution for stretchable neural interfaces.

In summary, here we report a stretchable neural interface using a conducting polymer film as the sole conductor for both electrodes and leads. This neural interface carries the benefits of conducting polymer electrodes in a demanding stretchable format. Electromechanical testing revealed that the stretchable interconnect could withstand uniaxial tensile strains up to  $(22.84 \pm 1.64)\%$  ( $n = 4$ ), while the resistance increased linearly with strain and peaked at an increase of only  $(16.10 \pm 0.92)\%$  at the rupture strain. This implies negligible disturbance to the electrode impedance from the stretchable interconnect by large strain loadings. Electrical impedance spectroscopy identified the SPMEA's advantage for recording LFPs, including EMG, ECG, ECoG and EEG. Cyclic voltammetry revealed impressive charge storage/injection capacities of the SPMEA, which is applicable for epimysial stimulation of denervated skeletal muscles. Future work from our group will include characterization of the long-term *in vivo* performance of the SPMEA as applied to epimysial recording and stimulation of denervated skeletal muscles during the course of peripheral nerve repair.

## Experimental

### Chemicals and Materials

All chemicals were purchased from Sigma-Aldrich unless otherwise indicated. Pyrrole and boron trifluoride diethyl etherate (BFEE) were distilled under reduced pressure prior to use. All the other chemicals were used without further purification. PolyCaprolactone-block-polyTetrahydrofuran-block-polyCaprolactone (PCTC) was purchased from Sigma-Aldrich (Catalog No. 526320) and characterized as  $CL_x-THF_y-CL_z$ ,  $x+z \approx 11$ ,  $y \approx 17$  [30]. OmniCoat, SU-8 2010, and SU-8 Developer were purchased from MicroChem Corp. NR-5 8000 Negative Photoresist was purchased from Futurrex, Inc. PDMS (Sylgard 184) was purchased from a distributor of Dow Corning Corp. Microscopy glass slides ( $2.5\text{ cm} \times 7.5$

cm × 1 mm) were purchased from VWR. Silver wires and stainless steel wires were purchased from A-M Systems.

### Electrochemical Synthesis of PPy/PCTC Composite Film

Electrochemical synthesis of PPy was performed in a one-compartment cell consisting of a 25 nm Pt-coated (with 10 nm Ti to enhance adhesion) glass electrode (2.5 cm × 4 cm × 1 mm) as the working electrode, a double-sided 1.5 cm × 2 cm stainless steel electrode as the counter electrode, and a 2.0 mm diameter Ag/AgCl wire (immersed directly in the solution) as the quasi-reference [12]. The experiments were controlled by a Model 263A Potentiostat–Galvanostat (EG&G Princeton Applied Research). The typical electrolyte was 0.05 M pyrrole in a mixture of isopropyl alcohol, boron trifluoride diethyl etherate at a volume ratio of 7:3, with 0.07 M PolyCaprolactone-block-polyTetrahydrofuran-block-polyCaprolactone (PCTC). The solution was degassed on a rotary evaporator at 15 kPa for 3 min. The electropolymerization was carried out at a constant current density of 0.8–1 mA cm<sup>−2</sup> at 0°C. After synthesis, the working electrode was rinsed briefly by isopropanol. The obtained PPy composite was referred to as PPy/PCTC (with PCTC in composition).

### SPMEA Fabrication

The fabrication process flow is shown in Figure S6. A 25 nm Pt-coated (with 10 nm Ti to enhance adhesion) glass slide (2.5 cm × 4 cm × 1 mm) was spin-coated with a thin OmniCoat layer and patterned with a 20 μm thick SU-8 mask to define the SPMEA electrodes, leads and contact pads. Following hard-baking of the sample on a 150°C hotplate for 30 min, the OmniCoat film in exposed windows of the SU-8 mask was removed by O<sub>2</sub> plasma etch (100 W, 500 mTorr, 5 min). One end of a short stainless steel wire (76.2 μm, A-M Systems) was placed in each contact pad window and all of the wires were fixed by a paper clamp through a piece of 25 μm thick glass band (not illustrated). PPy was electroplated in exposed windows of the patterned sample to produce electrodes, leads, and contact pads with a film thickness of ~15 μm. Afterward, only the portion of the sample with SPMEA contact pads and stainless steel wires was immersed in the electrolyte for extended electroplating to reinforce the connections. In this way, stainless steel wires in the contact pad windows were firmly integrated with the plated PPy material, resulting in a reliable, low contact-resistance connection to the PPy lead. The plated sample was then briefly rinsed with isopropanol and air dried.

Under a dissection microscope, the SU-8 mask was gently removed using a pair of fine tweezers, leaving the patterned PPy/PCTC layer on the glass slide. A piece of Blue Polyester Masking Tape was applied to the sample to peel the PPy/PCTC pattern off the Pt-coated glass slide. A gold-coated (5 nm gold with 1 nm Ti for adhesion) glass slide with a 125 μm PDMS base layer spin-coated and cured on top was prepared separately. The polyester tape together with the PPy/PCTC pattern was soaked in 5% 3-amino-propyltriethoxysilane (APTES) water solution (by volume) [20] at room temperature for 20 min, rinsed briefly with DI water and air dried. Fine NaCl powder was applied to the tape to block the adhesives, and then the powder on PPy/PCTC was gently wiped off by Texwipe (the powder didn't stick to the smooth PPy/PCTC surface and could be wiped off completely). Then both the tape and PDMS base layer on the gold-coated glass slide were treated by air plasma (200

W, 200 mTorr) for 1 min to activate the PPy/PCTC and PDMS surfaces. After treatment, the two parts were immediately brought together to form irreversible bonding between the PPy/PCTC pattern and PDMS base layer. With isopropyl alcohol wetting, the tape was easily peeled off, completely transferring the entire PPy/PCTC pattern to the PDMS base layer. Residual NaCl powder on the PDMS surface was dissolved and rinsed away by DI water. The sample was then cleaned by ethanol and DI water washes.

Subsequently, the sample underwent passivation [21]. Sacrificial posts (NR5-8000, Futurrex, Inc.) were patterned on the PPy/PCTC electrodes and the sample was soaked in 10% HCl solution for 5 min to balance the basic effects of APTES and RD6 Developer on PPy/PCTC interconnects [28]. A second 10  $\mu$ m PDMS layer was spin-coated to encapsulate the device. Sacrificial posts were then dissolved in acetone to expose the electrodes, and the sample was soaked in 10% HCl solution again for 5 min to restore the electromechanical properties of the PPy/PCTC electrodes. Finally, the finished device was peeled off the glass slide carrier.

### Interconnect Fabrication

2 cm  $\times$  1mm interconnects used for stretching experiments were fabricated using the same processes as the SPMEA. For bare PPy/PCTC interconnects, Steps (a) through (c) in Figure S6 were followed, and the interconnects were then peeled off the Pt-coated glass electrode. For stretchable interconnects with contact pads at both ends, the complete process in Figure S6 was employed and the interconnects were cut out of the final device with a razor blade.

### Conductivity Measurement

The electrical conductivity of dried PPy/PCTC films was measured using a standard four-point method, yielding a value  $116.3 \pm 7.8 \text{ S cm}^{-1}$  ( $n = 4$ ) at room temperature, which is typical for electrochemically synthesized PPy samples [1,2].

### Stretching Experiment

The stretching experiments were performed on an Instron Model 5943 Materials Testing System with a 50 N load cell stress sensor. All tests were carried out at 24°C and relative humidity of 60%, with no detectable air flow. The setup is shown in Figure S2. Briefly, a piece of 50  $\mu$ m thick copper foil was fixed to the inner side of each rubberized grip pad by a piece of double-sided tape to electrically interface to the specimen, which was clamped at each end by the grips. An insulated silver wire (200  $\mu$ m diameter, terminal stripped) was soldered to the edge of each piece of copper foil to make connection to one probe of a Fluke 45 digital multimeter, which was controlled by FlukeView Forms running on a computer for resistance recording. Each specimen was stretched at a rate of 0.1% strain per second and the resistance was sampled at 1 Hz.

### Electrical Impedance Spectroscopy

Electrical Impedance Spectroscopy was performed using a Solartron 1255B Frequency Response Analyzer coupled with a Solartron SI 1287 Electrochemical Interface. A standard three-electrode electrochemical cell was used, consisting of the testing SPMEA electrode as the working electrode, a 25 nm Pt-coated (with 10 nm Ti to enhance adhesion) glass

electrode as the counter electrode, and a 2.0 mm diameter Ag/AgCl wire as the quasi-reference (Figure S8). The experiment was controlled by ZPlot and ZView software (Scribner Associates, Inc.). A 10 mV voltage was applied, while the frequency was swept from 100 kHz to 0.1 Hz.

### Cyclic Voltammetry

The same three-electrode electrochemical cell as shown in Figure S8 was used. The experiment was controlled by a CHI760D potentiostat (CH Instruments, Inc.). Voltage scan rates of 50 mV s<sup>-1</sup> and 1 V s<sup>-1</sup> were used between the water electrolysis window of -0.6 V~0.8 V for the slow and fast CVs, respectively.

### Acute Recording Experiment

All experimental procedures were conducted in accordance with the guidelines of the Animal Care and Use Review Office (ACURO) of the USAMRMC Office of Research Protections (ORP) and the Committee on Animal Care of the Massachusetts Institute of Technology. One adult Lewis rat was anesthetized under continuous isoflurane (2%)/oxygen. The gastrocnemius muscle and sciatic nerve on the left side were dissected. The SPMEA was placed on the lateral gastrocnemius; the reference electrode was clamped on the flipped-over biceps femoris; and the ground electrode was clamped to the tail. The setup is shown in Figure 3d. The sciatic nerve was squeezed by a pair of fine tweezers and the EMG responses were amplified by a Brownlee Precision Model 440 Instrumentation Amplifier (gain = 1000, lowpass = 1 kHz, and highpass = 0.15 Hz) and digitized by a National Instruments USB-6353 DAQ system at 2 kHz. The animal was euthanized directly after the experiment. Offline data processing was done with Matlab 7.0 (MathWorks, Inc.) and a fourth-order Butterworth bandpass filter (1 Hz ~ 800 Hz) was applied to the raw data.

### Supplementary Material

Refer to Web version on PubMed Central for supplementary material.

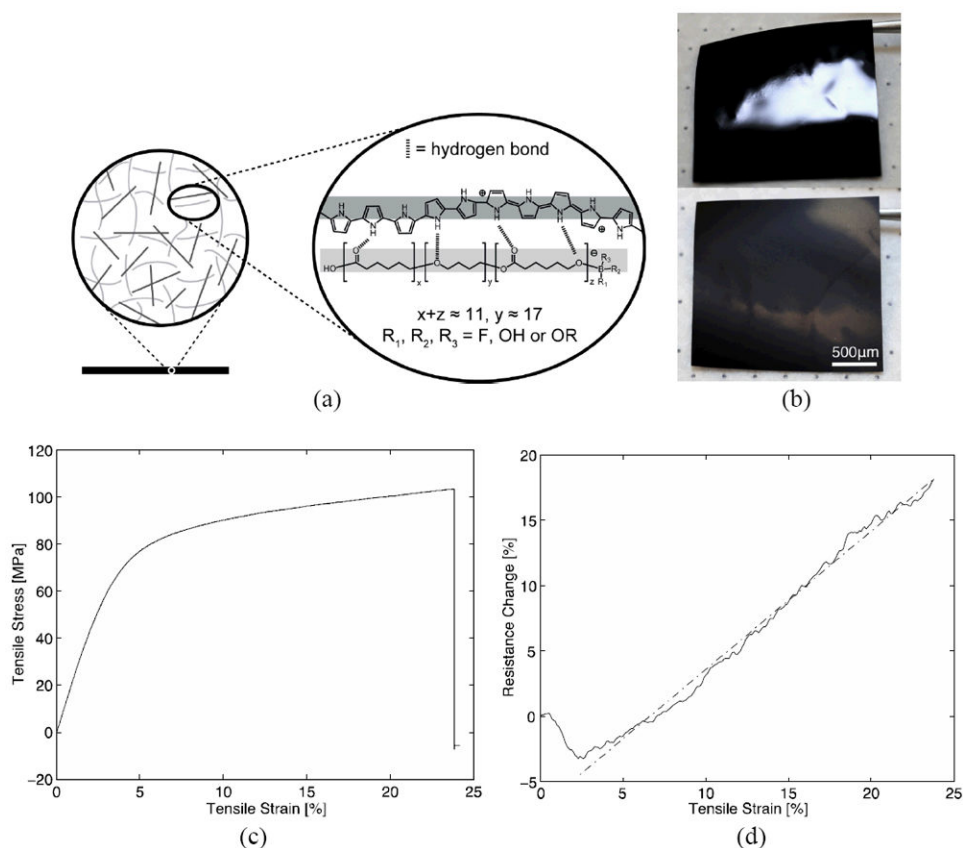
### Acknowledgments

This research was supported by the Armed Forces Institute of Regenerative Medicine (Contract No. W81XWH-08-2-0034), the National Heart, Lung, and Blood Institute (Program of Excellence in Nanotechnology (PEN) Award, Contract No. HHSN268201000045C), and the National Cancer Institute (Grant No. CA151884). We thank Drs. M. A. Invernale and B. L. Larson for valuable comments on the manuscript.

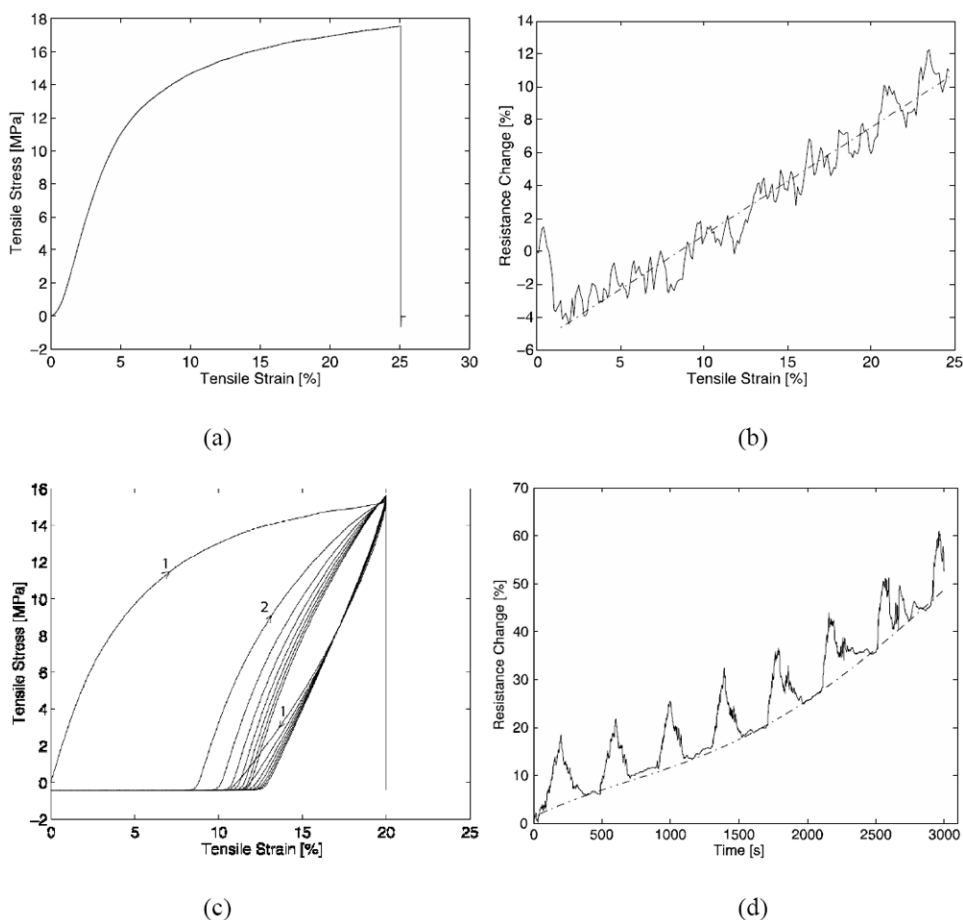
### References

1. Green RA, Lovell NH, Wallace GG, Poole-Warren LA. Biomaterials. 2008; 29:3393. [PubMed: 18501423]
2. Guimard NK, Gomez N, Schmidt CE. Prog Polym Sci. 2007; 32:876.
3. a) Ravichandran R, Sundarrajan S, Venugopal JR, Mukherjee S, Ramakrishna S. J R Soc Interface. 2010; 7:S559. [PubMed: 20610422] b) Ateh DD, Navsaria HA, Vадgama P. J R Soc Interface. 2006; 3:741. [PubMed: 17015302]
4. Green RA, Baek S, Poole-Warren LA, Martens PJ. Sci Technol Adv Mater. 2010; 11 014107.
5. Abidian MR, Martin DC. Biomaterials. 2008; 29:1273. [PubMed: 18093644] b) Abidian MR, Ludwig KA, Marzullo TC, Martin DC, Kipke DR. Adv Mater. 2009; 21:3764.c) Abidian MR, Corey JM, Kipke DR, Martin DC. Small. 2010; 6:421. [PubMed: 20077424]

6. a) Schmidt CE, Shastri VR, Vacanti JP, Langer RS. *Proc Natl Acad Sci USA*. 1997; 94:8948. [PubMed: 9256415] b) Gomez N, Lee JY, Nickels JD, Schmidt CE. *Adv Funct Mater*. 2007; 17:1645. [PubMed: 19655035]
7. Liu X, Gilmore KJ, Moulton SE, Wallace GG. *J Neural Eng*. 2009; 6 065002.
8. George PM, Lyckman AW, LaVan DA, Hegde A, Leung Y, Avasare R, Testa C, Alexander PM, Langer R, Sur M. *Biomaterials*. 2005; 26:3511. [PubMed: 15621241]
9. a) Blau A, Murr A, Wolff S, Sernagor E, Medini P, Iurilli G, Ziegler C, Benfenati F. *Biomaterials*. 2011; 32:1778. [PubMed: 21145588] b) Blau, A. *Applied Biomedical Engineering*. Gargiulo, GD.; McEwan, A., editors. Vol. Ch. 5. InTech; 2011.
10. Keohan F, Wei XF, Wongsarnpigoon A, Lazaro E, Darga JE, Grill WM. *J Biomater Sci Polymer Edn*. 2007; 18:1057.
11. Khodagholy D, Doublet T, Gurfinkel M, Quilichini P, Ismailova E, Leleux P, Herve T, Sanaur S, Bernard C, Malliaras GG. *Adv Mater*. 2011; 23:H268. [PubMed: 21826747]
12. Ma M, Guo L, Anderson DG, Langer RS. *Science*. 2013; 339:186. [PubMed: 23307738]
13. Zheng W, Alici G, Clingan PR, Munro BJ, Spinks GM, Steele JR, Wallace GG. *J Polym Sci B Polym Phys*. 2013; 51:57.
14. Tjahyono AP, Aw KC, Travas-Sejdic J. *Sens Actuators B*. 2012; 166:426.
15. a) Oh EJ, Jang KS, Park SY, Han SS, Suh JS. *Mol Cryst Liq Cryst*. 2001; 371:243. Oh EJ, Jang KS, MacDiarmid AG. *Synth Met*. 2002; 125:267.
16. a) Shi G, Jin S, Xue G, Li C. *Science*. 1995; 267:994. [PubMed: 17811437] b) Xu J, Shi G, Qu L, Zhang J. *Synth Met*. 2003; 135:221.
17. Li T, Suo Z. *Int J Sol Struct*. 2006; 43:2351.
18. a) Lacour SP, Jones JE, Wagner S, Li T, Suo Z. *Proc IEEE*. 2005; 93:1459. b) Wagner S, Lacour SP, Jones J, Hsu PI, Sturm JC, Li T, Suo Z. *Physica E*. 2004; 25:326.
19. a) Li T, Huang Y, Xi Z, Lacour SP, Wagner S, Suo Z. *Mech Mater*. 2005; 37:261. b) Xia Y, Li T, Suo Z, Vlassak JJ. *Appl Phys Lett*. 2005; 87:161910.
20. Aran K, Sasso LA, Kamdar N, Zahn JD. *Lab Chip*. 2010; 10:548. [PubMed: 20162227]
21. a) Guo L, Meacham KW, Hochman S, DeWeerth SP. *IEEE Trans Biomed Eng*. 2010; 57:2485. [PubMed: 20550983] Guo L, Guvanasen GS, Liu X, Tuthill C, Nichols TR, DeWeerth SP. *IEEE Trans on Biomed Cir and Sys*. 2013; 7:1.
22. Cogan SF. *Annu Rev Biomed Eng*. 2008; 10:275. [PubMed: 18429704]
23. Mayr W, Hofer C, Bijak M, Rafolt D, Unger E, Reichel M, Sauermann S, Lanmueller H, Kern H. *Basic Appl Myol*. 2002; 12:287.
24. Lanmüller H, Ashley Z, Unger E, Sutherland H, Reichel M, Russold M, Jarvis J, Mayr W, Salmons S. *Med Biol Eng Comput*. 2005; 43:535. [PubMed: 16255438]
25. Maghribi, M.; Hamilton, J.; Polla, D.; Rose, K.; Wilson, T.; Krule-vitch, P. *Proc 2nd Annu Int IEEE-EMB Special Topic Conf Microtechnologies in Medicine and Biology*; 2002. p. 80
26. Lacour, SP.; Tsay, C.; Wagner, S.; Yu, Z.; Morrison, B. *Proc 4th IEEE Sensors Conf*; 2005. p. 617
27. Schuettler M, Stiess S, King BV, Suanning GJ. *J Neural Eng*. 2005; 2:S121. [PubMed: 15876647]
28. a) Münstedt H. *Polymer*. 1986; 27:899. b) Sun B, Jones JJ, Burford RP, Skyllas-Kazacos M. *J Mater Sci*. 1989; 24:4024.
29. a) Wilks SJ, Richardson-Burns SM, Hendricks JL, Martin DC, Otto KJ. *Front Neuroeng*. 2009; 2 Article 7. b) Venkatraman S, Hendricks J, King ZA, Sereno AJ, Richardson-Burns S, Martin D, Carmena JM. *IEEE T Neur Sys Reh*. 2011; 19:307.
30. Li J, Chen B, Wang X, Goh SH. *Polymer*. 2004; 45:1777.
31. Bae WJ, Ruddy BP, Richardson AG, Hunter IW, Bizzi E. *Proceedings of IEEE EMBS*. 2008:5794.
32. Byun I, Coleman AW, Kim B. *J Micromech Microeng*. 2013; 23 085016.

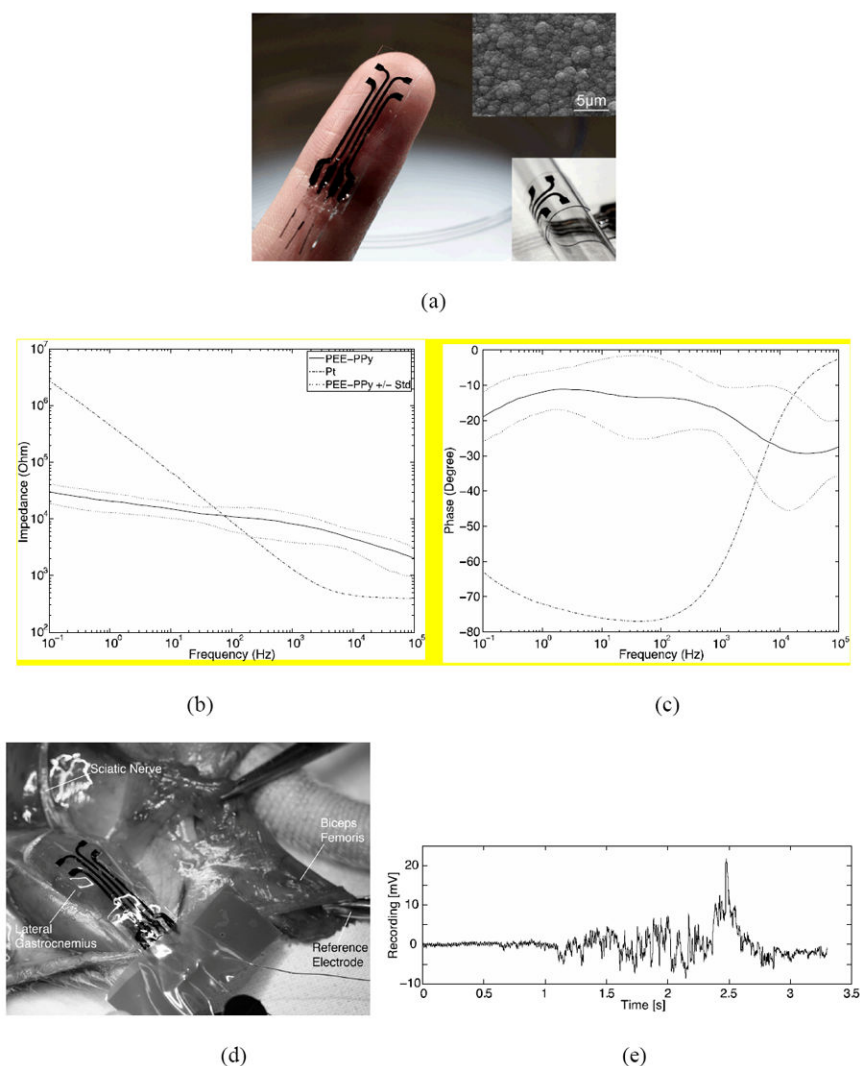


**Figure 1.** PPy/PCTC composite and electromechanical properties in the dry state. (a) Schematic of the PPy/PCTC composite structure. A PPy/PCTC composite film (black) is composed of PPy polymer chains (dark grey lines) and a polyol-borate network (light grey lines). (b) Photographs of a 15  $\mu\text{m}$  thick PPy/PCTC composite film showing different surface smoothness on two sides: top, the side facing the Pt electrode; bottom, the side facing the plating solution (an SEM image of the surface is shown in the top inset of Figure 3a). (c) Representative stress-strain curve of a PPy/PCTC specimen (see Figure S2 for the stretching setup) with an ultimate tensile strain of 24% (ultimate tensile strength 103.48 MPa; Young's Modulus 128.9 MPa). The test was performed in 60% humidity ambient condition, when the specimen had reached equilibrium in a dry state with the surrounding air. (d) Resistance-strain curve (solid line) of the specimen in (c). The curve was fitted by a linear function (dash-dotted line, see Supporting Information). The initial curve shows a sag of the contact resistance between the specimen and electrodes.



**Figure 2.**

Electromechanical testing of stretchable interconnects. (a) Representative stress-strain curve of a stretchable interconnect breaking at 24.8% tensile strain. (b) Resistance-strain curve (solid line) of the stretchable interconnect in (a). The curve was fitted by a linear function (dash-dotted line, see Supporting Information). The initial curve shows a sag of the contact resistance between the specimen and electrodes. (c) Stress-strain plot of a stretchable interconnect during 20% cyclic strain, which broke after 7.5 cycles. The first two cycles are marked by arrows. (d) Resistance-strain plot (solid line) of the stretchable interconnect in (c). The baseline was fitted by a polynomial function (dash-dotted line, see Supporting Information).

**Figure 3.**

Characterization of the SPMEA for neural recording. (a) Image of the SPMEA. The electrode opening was 1 mm in diameter (see Figure S7 for optical microscopic images of an electrode) and the leads were 0.5 mm wide. Top inset: SEM image of the electrode surface; bottom inset: the device was conformably wrapped around a 6.5 mm diameter glass pipette. (b) and (c) Average electrical impedance spectrum with standard deviation of the four electrodes. A Pt disc electrode (see Figure S9) of the same geometric surface area was used as a control. (d) Experimental setup for epimysial recording with a rat model. The SPMEA was placed on the lateral gastrocnemius, while the reference electrode was clamped on the biceps femoris. (d) A representative recording trace following a mechanical squeeze of the sciatic nerve. The FFT of this signal is shown in Figure S10.

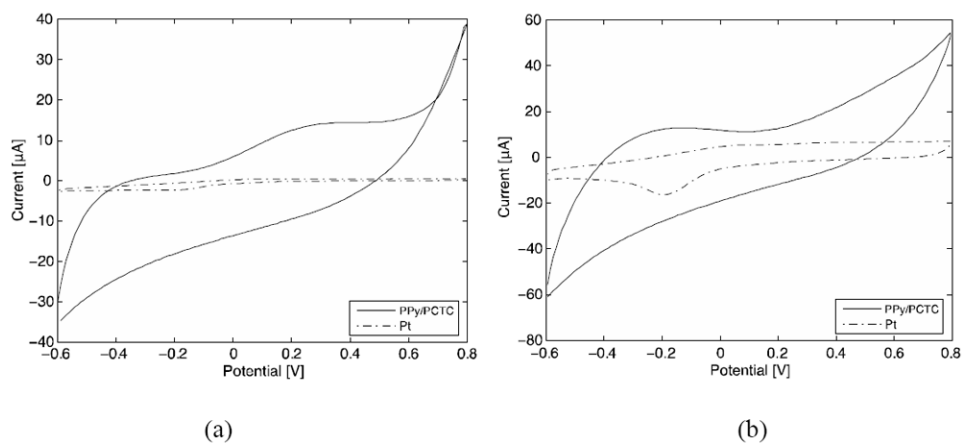


**Figure 4.**

Characterization of the SPMEA for neural stimulation. (a) Cyclic voltammograms of one SPMEA electrode and one Pt disc electrode at a voltage scan rate of 50 mV s<sup>-1</sup> within the water electrolysis window. The cathodic charge storage capacity of the PPy/PCTC electrode is -48.8 mC cm<sup>-2</sup>; and that of the Pt electrode is -5.0 mC cm<sup>-2</sup>. (b) Cyclic voltammograms at a scan rate of 1 V s<sup>-1</sup>. The cathodic charge transfer was: PPy/PCTC, -3.9 mC cm<sup>-2</sup>; Pt, -1.1 mC cm<sup>-2</sup>.